

Optimal Strategies for Free Flight Air Traffic Conflict Resolution*

By

P. K. Menon and G. D. Sweriduk

Optimal Synthesis

450 San Antonio Road, Suite 46

Palo Alto, CA 94306-4638

(415) 494 - 7569

B. Sridhar

NASA Ames Research Center

Moffett Field, CA 94035-1000

* Research Supported under NASA Contract NAS1-14333

Abstract

Recent advances in navigation and data communication technologies make it feasible for individual aircraft to plan and fly their trajectories in the presence of other aircraft in the airspace. This way, individual aircraft can take advantage of the atmospheric and traffic conditions to optimally plan their paths. This capability is termed as the *free flight* concept. While the free flight concept provides new degrees of freedom to the aircraft operators, it also brings-in complexities not present in the current air traffic control system. In the free flight concept, each aircraft has the responsibility for navigating around other aircraft in the airspace. While this is not a difficult task under low speed, low traffic density conditions, the complexities of dealing with potential conflict with multiple aircraft can significantly increase the pilot's work load.

This paper presents the development of a conflict resolution algorithm based on the quasi-linearization method to enable the practical implementation of the free flight concept. The algorithm development uses nonlinear point-mass aircraft models, and incorporates realistic operational constraints on individual aircraft. The analytical framework can also incorporate information about ambient atmospheric conditions. Realistic conflict resolution scenarios are illustrated. Due to their speed of execution, these conflict resolution algorithms are suitable for implementation on-board aircraft.

1. Introduction

Recent advances in Global Positioning System (GPS) - based navigation techniques and satellite data communications technology have motivated the FAA and commercial air traffic carriers to consider the "free flight" concept as a major component of the future air traffic control system [1, 2]. Free flight is defined as safe and efficient flight operations under instrument flight

rules in which the operators have the freedom to select their path and speed in real time. Thus, individual aircraft will be able to plan and execute their trajectories without direction from any external agents during most of their flight duration. The ability of individual aircraft to plan their trajectories can result in substantial improvements in operational efficiency, since the aircraft can take advantage of atmospheric and traffic conditions to minimize the delays and fuel consumption. This approach can also lead to optimal coordination between aircraft involved in hub/spoke modes of operation currently employed by most major air carriers. However, since different aircraft in a given airspace may have conflicting objectives, the desired trajectories synthesized by individual aircraft can generate conflicts with other aircraft trajectories. Successful implementation of the free flight concept will require the development of systematic methods for multi-aircraft conflict resolution. While conflict resolution strategies are obvious under low speed, low traffic density conditions, the problem can become complex as the traffic density and the aircraft speeds increase. This fact has motivated several research studies on various aspects of the free-flight conflict resolution problem at NASA and other research centers [3 - 10].

The focus of the research effort described in this paper is on the development of systematic methods for multiple aircraft conflict resolution. Conflict resolution algorithms employed in the present air traffic management automation tools are largely rule-based, and are designed to operate under the existing air traffic control procedures [11 - 15]. While these methods are adequate for resolving simultaneous conflicts between aircraft following standard jet routes, it is not clear how these methods can be generalized to handle multiple aircraft conflicts that can arise in the free flight environment. The emphasis of the research reported in this paper is in formulating and solving the conflict resolution problem as a trajectory optimization problem. As with other aerospace guidance problems, application of optimal control theory [16] and differential game theory [17] will result in more systematic methodologies for the solution of the conflict resolution problem. This fact has been demonstrated in several recent aerospace trajectory synthesis problems [18 - 22]. Unlike rule-based conflict resolution approaches, one of the advantages of the formalism presented here is that the same algorithms are independent of the conflict resolution geometry. Present research builds upon a previous research effort [5, 23] on the conflict resolution problem.

Conflict resolution methodologies developed in the present research assume that each aircraft trajectory involved in a potential conflict is given by a sequence of 4 dimensional (three position

coordinates and time) waypoints. Nominal waypoint sequences are adjusted by the conflict resolution algorithm in order to synthesize conflict-free trajectories that optimize desired performance indices. The conflict resolution problem is formulated both as a single objective optimization problem and as a multiple objective optimization problem [24, 25]. Various types of curves can be used to define the actual aircraft trajectory between the waypoints. The use of piecewise linear and cubic spline trajectories are both considered in the present research. Inter-aircraft conflict is defined through a conflict envelope in the form of an oblate spheroid.

The trajectory optimization formulation uses nonlinear point-mass models of aircraft with realistic aerodynamic and engine models [26, 27]. Two different cost functions are used in this study: a linear combination of total flight time and fuel consumption, and integral square of the perturbation from nominal trajectories. The latter function assumes that the nominal trajectories have already been optimized by each individual aircraft, and that the conflict resolution methodology should only perturb these trajectories by the smallest amount required to accomplish conflict resolution. The advantage of the latter formulation is that individual aircraft need not reveal their core trajectory planning strategies to other aircraft involved in the conflict resolution process. The constraints employed in the present formulation are: inter-aircraft distance, maximum and minimum airspeeds, maximum climb and descent rates, maximum and minimum altitude limits, maximum bank angle, maximum and minimum load factors, and maximum and minimum thrusts limits. Vehicle models, constraints, and trajectory parameterization schemes are discussed in Section 2.

Iterative numerical methods and semi-analytical guidance laws are developed based on trajectory optimization theory [16]. Iterative methods that formulate the conflict resolution problem as a single objective optimization problem, and as multiple objective optimization problem are given in Section 3. Semi-analytical guidance law development using quasi-linearization is presented in Section 4. Several conflict resolution scenarios are given in Sections 3 and 4 to illustrate the performance of these algorithms. In every case, it is shown that the methods produce useful conflict resolution strategies. Further, the results show that the conflict resolution algorithms developed in the present research are general enough to handle every type of conflict that can occur in the free flight air transportation environment. Conclusions from the present research effort and future research issues are given in Section 5.

2. Aircraft, Trajectory, and Conflict Envelope Models

Three major components of the conflict resolution problems analyzed in the present research are the aircraft models, trajectory parameterization schemes, and conflict envelope definitions. Efficiency of the conflict resolution algorithms can be greatly enhanced by using appropriate aircraft models and trajectory parameterization schemes. The computational efficiency of implementing aircraft operational constraints can be improved by employing appropriate transformations on the aircraft models. Careful definition of the inter-aircraft conflict envelopes can further improve the conditioning of the conflict resolution problem. Each of these issues are discussed in the following subsections.

2.1. Aircraft Models

Point-mass aircraft models are used in the present research. The point-mass aircraft model captures most of the dynamical effects encountered in civil aviation aircraft. These models are popular in aircraft performance work, and are used in practically every aircraft trajectory optimization problem discussed in the literature. The point-mass equations of motion are formulated with respect to a coordinate system shown in Figure 1.

The point-mass model assumes that the aircraft thrust is directed along the velocity vector, and that the aircraft always performs coordinated maneuvers. It further assumes a flat, non-rotating earth. These assumptions are reasonable for civil aviation aircraft operating within a range of 200 nautical miles. Since the conflict resolution generally occurs within this range, the fidelity provided by the point-mass model is adequate for formulating these problems. Note that it is feasible to develop point mass models valid for spherical earth approximations also. The point-mass aircraft equations describing aircraft flight are:

$$\dot{V}_i = \frac{(T_i - D_i)}{m_i} - g \sin \gamma_i \quad \dot{\gamma}_i = \frac{g}{V_i} \left(\frac{L_i \cos \phi_i}{g m_i} - \cos \gamma_i \right) \quad \dot{\chi}_i = \frac{L_i \sin \phi_i}{m_i V_i \cos \gamma_i} \quad (1)$$

$$m_i = - Q_i \quad (2)$$

$$\dot{x}_i = V_i \cos \gamma_i \cos \chi_i \quad \dot{y}_i = V_i \cos \gamma_i \sin \chi_i \quad \dot{h}_i = V_i \sin \gamma_i \quad (3)$$

with $i = 1, 2, \dots, n$ being the aircraft under consideration. In these equations, and V_i is the ground speed, assumed to be equal to airspeed during the present research. T_i is the aircraft engine thrust,

D_i is the drag, m_i is the aircraft mass, g is the acceleration due to gravity, γ_i is the flight path angle, L_i is the vehicle lift, ϕ_i is the bank angle, χ_i is the aircraft heading angle, x_i is the down range, y_i is the cross range, h_i is the altitude, and Q_i is the fuel flow rate. The fuel flow rate depends on the altitude, Mach number and the engine thrust. The aircraft drag is given in terms of the zero-lift drag coefficient, and induced drag coefficient. Both of these are specified as functions of Mach number and the aircraft configuration setting such as the deployment of flaps, speed brakes, and the landing gear. For the present research, it is assumed that the aircraft is in the cruise flight configuration. The control variables in the aircraft model are the load factor n_i controlled using the elevator, the bank angle ϕ_i controlled using a combination of rudder and ailerons, and the engine thrust T_i controlled using the throttle. Throughout the conflict resolution process, the control variables will be constrained to remain within specified limits.

For analytical convenience, the kinematic equations describing the aircraft position can be differentiated once with respect to time, and the remaining dynamic equations can be used to cast the point-mass aircraft model in an alternate form as:

$$\ddot{\mathbf{x}} = U_1 \ddot{\mathbf{y}} = U_2 \ddot{\mathbf{h}} = U_3 \quad (4)$$

U_1 , U_2 , U_3 are the three new control variables in the point mass model. The relationship between these control variables and the actual control variables is given by the expressions [28]:

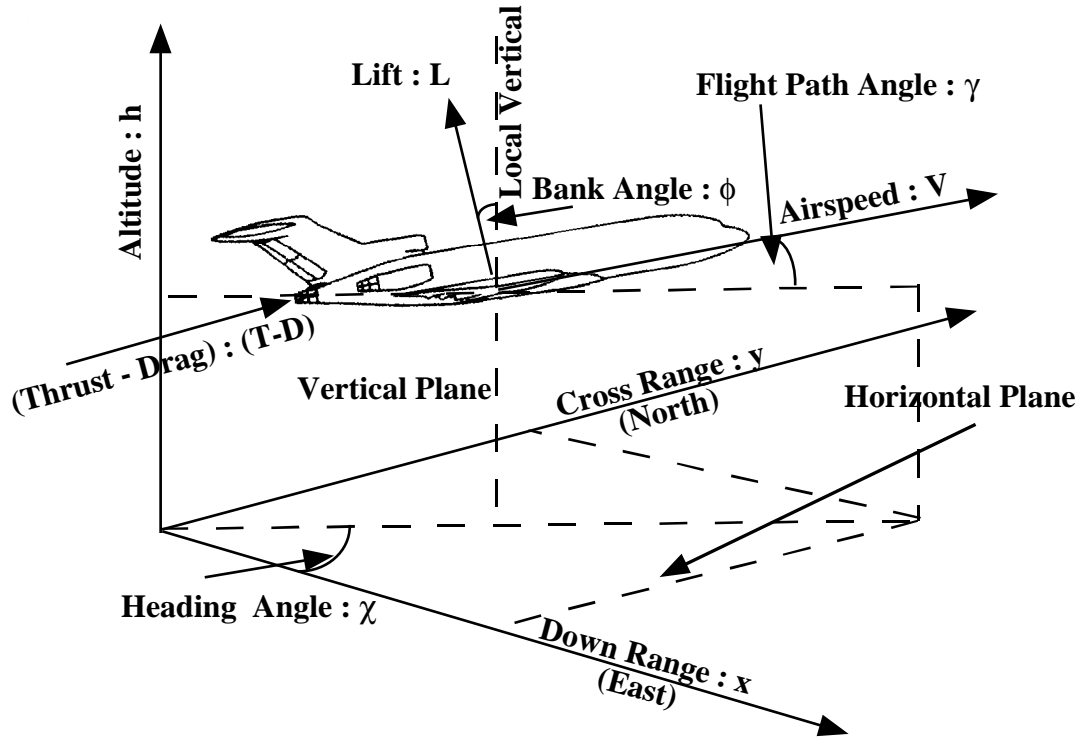


Fig. 1 . The Aircraft Coordinate System

$$\phi = \tan^{-1} \left[\frac{U_2 \cos \chi - U_1 \sin \chi}{\cos \gamma (U_3 + g) - \sin \gamma (U_1 \cos \chi + U_2 \sin \chi)} \right] \quad (5)$$

$$n = \frac{\cos \gamma (U_3 + g) - \sin \gamma (U_1 \cos \chi + U_2 \sin \chi)}{g \cos \phi} \quad (6)$$

$$T = [\sin \gamma (U_3 + g) + \cos \gamma (U_1 \cos \chi + U_2 \sin \chi)] m + D \quad (7)$$

the heading angle χ and the flight path angle γ are computed as:

$$\tan \chi = \frac{\dot{y}}{\dot{x}} \quad \sin \gamma = \frac{\dot{h}}{V} \quad (8)$$

This latter form of aircraft point-mass model is useful for mapping geometric trajectory parameters in terms of the aircraft control variables, and vice-versa. Thus, constraints on the aircraft control variables can be readily transformed into constraints on the trajectory curvature. Such mappings are useful for efficient implementation of control constraints, as will be demonstrated in subsequent sections.

2.2. Trajectory Parameterization

Trajectory parameterization methods allow the description of individual aircraft trajectories using a small number of parameters. In addition to providing a compact description of the trajectories, trajectory parameterization methods permit the solution of the trajectory optimization problems as parameter optimization problems. Parameterized aircraft trajectories are described using a set of four-dimensional waypoints consisting of three position components and time, together with the specification of the type of curves joining them. Two types of trajectory parameterization schemes are used in the present research. These are piecewise linear trajectories and cubic spline trajectories. Piecewise linear trajectory parameterization is highly efficient from a computational standpoint. However, the piecewise linear trajectory parameterization implies abrupt changes in aircraft control variables at the waypoints. Since such abrupt control variations are not desirable, smooth trajectory segments will need to be introduced in the vicinity of the waypoints to ensure practical implementability. Note that these trajectory segments can introduce uncertainties in the aircraft position near the way points. It is assumed in the present research that these smooth trajectory segments can be introduced without adversely affecting the conflict resolution solutions.

On the other hand, the cubic spline parameterization produces smooth trajectories as well as smooth control settings. The disadvantage of this parameterization scheme is that it requires more computation time, and that it tends to introduce anomalies in the path by virtue of its fitting a fixed-order smooth curve through a given set of points. Due to these factors, although a few cubic spline parameterization cases were studied during the present research, the emphasis is on the use of piecewise linear trajectory parameterization.

2.3. Conflict Envelope Definition

According to the currently accepted definition [12], a conflict is said to occur if the altitude difference between an aircraft pair occupying the same down-range, cross-range coordinates is

less than 2000 feet; or if the two aircraft are closer than 5 nautical miles while flying at the same altitude. It is convenient to conceptualize these requirements by imagining that each aircraft is centered inside a hypothetical conflict box with dimensions of 10 nautical miles length and breadth with 4000 feet thickness. Any other aircraft entering this hypothetical box can be considered as causing a conflict.

Although this definition of a conflict is simple to conceptualize, it can cause severe numerical difficulties due the corners present in such a conflict envelope. For instance, in certain kinematic conflict configurations, small motion of the aircraft can cause a large change in the conflict status. Such large changes can cause numerical instabilities in the conflict resolution algorithm. Alternate definitions can be developed to enforce the aircraft separation constraint without introducing such numerical discontinuities. Possibilities include quadratic surfaces [30] and super quadric surfaces [31, 32]. An oblate spheroidal conflict envelope is an example of a quadratic surface. The oblate spheroidal conflict envelope has an elliptical cross section in the vertical plane, and a circular cross section in the horizontal plane. In order to approximate the FAA definition of the conflict envelope, the semi-major axis of the elliptical cross section can be chosen as 5 nautical miles, and the semi-minor axis can be set at 2000 feet. A schematic view of the oblate spheroidal conflict envelope in the vertical plane is shown in Figure 2 for a pair of aircraft.

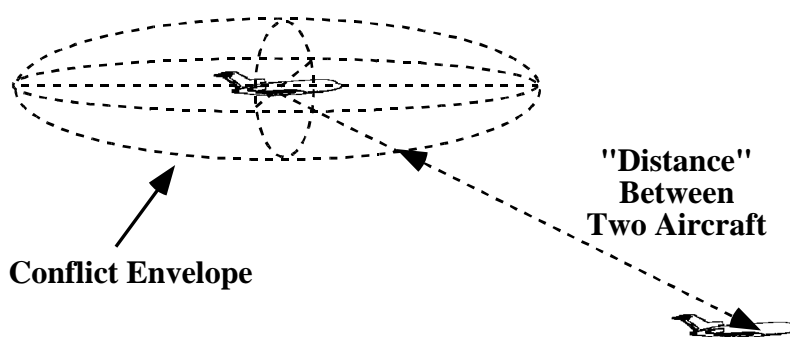


Fig. 2 . Oblate Spheroidal Conflict Envelope and the Inter-Aircraft Distance in the Vertical Plane

Figure 3 shows the definition of the oblate spheroid conflict envelopes for three aircraft in the horizontal plane. Note that the “inter-aircraft distance” is the distance from an aircraft’s CG to another aircraft’s conflict envelope.

Using this geometry, the distance $r_{i,j}$ between any two aircraft i, j can be defined using the expression:

$$r_{i,j} = \sqrt{\Delta x_{i,j}^2 + \Delta y_{i,j}^2 + \Delta h_{i,j}^2} - \sqrt{\frac{a^2 b^2 (\Delta x_{i,j}^2 + \Delta y_{i,j}^2 + \Delta h_{i,j}^2)}{a^2 \Delta h_{i,j}^2 + b^2 (\Delta x_{i,j}^2 + \Delta y_{i,j}^2)}}, i \neq j \quad (9)$$

In this expression, a is the conflict envelope semi-major axis, b is the semi-minor axis, and $\Delta x_{i,j}$, $\Delta y_{i,j}$, $\Delta h_{i,j}$ are the components of the relative position vector between any two aircraft i and j . It can be verified that if $a = b$, the conflict envelope degenerates into a sphere. Further, it can be shown that $r_{i,j} = r_{j,i}$. A conflict can be defined as a situation in which any of the inter-aircraft distances $r_{i,j}$ fall below zero. Note that if n aircraft are involved in an air traffic control situation, a maximum of $n(n-1)/2$ conflicts can simultaneously arise. The resulting inter-aircraft distances can be represented as a symmetric matrix with zeros along the diagonal. Any conflict resolution methodology must ensure that all the off-diagonal elements of the inter-aircraft distance matrix remain above zero at all times. A further refinement of the inter-aircraft conflict definition is to introduce a matrix norm in the formulation. The Frobenius norm or the Matrix 2 norm [33] is a candidate measure that can be used to express the inter-aircraft conflict in a compact form.

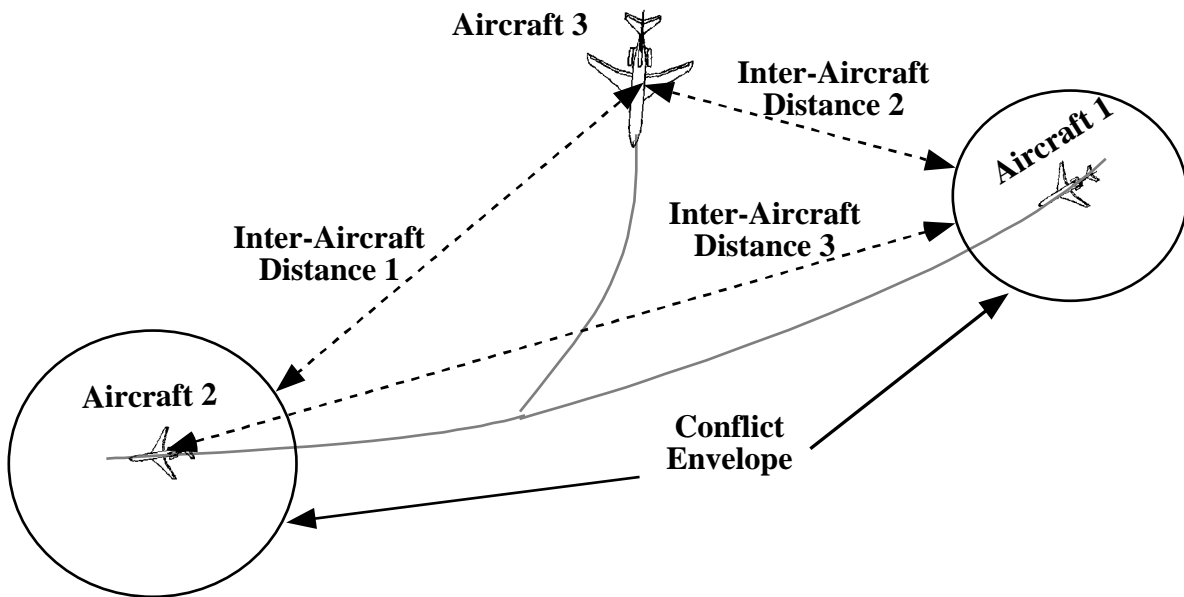


Fig. 3 . Definition of the “Inter-Aircraft Distance” in the Horizontal Plane

3. Direct Iterative Methods for Conflict Resolution

The conflict resolution process consists of modifying the aircraft nominal airspeed, altitude, down-range and cross range trajectory components to ensure that every aircraft stays out of the every other aircraft's conflict envelope while executing their flight plans. These trajectory perturbations must not significantly change the arrival times at the specified terminal point, and should not result in excessive maneuvering. Moreover, conflict resolution trajectory changes should be such that they do not lead to future conflicts. In some cases, it may be desirable to include fuel conservative measures in the conflict resolution performance objectives. Since the atmospheric perturbations and piloting techniques introduce uncertainties in the aircraft trajectories, the trajectory synthesis should be such that the worst-case perturbations in each aircraft trajectory still preserve the integrity of the conflict resolution process.

From the foregoing requirements, it can be observed that the conflict resolution problem can be formulated as a multi-participant trajectory optimization problem. This problem can be cast in several different forms by assigning roles to individual aircraft. For instance, it can be treated as a single objective trajectory optimization problem in which every aircraft performs conflict resolution maneuvers that optimize a defined performance index. Alternatively, the conflict resolution problem can be cast as a series of one-sided optimal control problems by considering a pair of aircraft at a time, with one aircraft operating along the nominal trajectory, and the other aircraft making the necessary trajectory adjustments required for conflict resolution. Finally, it can be treated as a multi-objective optimization problem in which each participant makes the least amount of trajectory deviations necessary for maintaining the inter-aircraft distance above a minimum specified value while simultaneously optimizing its performance criterion. Such approaches to the conflict resolution problem can be considered as a "cooperative conflict resolution approach". Other variations of the conflict resolution problem formulation are presented in the Section 4.

All these approaches require the definition of performance indices that reflect the operational requirements of the conflict resolution problem. Performance indices considered in the present research are linear combinations of flight time and fuel, and integral square of the deviations from the nominal flight paths. The constraints in the problem include the minimum permissible inter-aircraft separation and aircraft performance limits. Additionally, aircraft trajectories may be

required to pass through a series of metering waypoints, as is required in the current air traffic control environment. The resulting problem is a state constrained optimal control problem [16, 17] that can be approached using well developed mathematical techniques.

The necessary conditions for the optimality of state constrained optimal control problems result in multi-point boundary-value problems. There are two major families of techniques useful for solving these problems. Firstly, the conflict resolution problem can be converted into a parameter optimization problem by parameterizing the trajectories. Trajectory parameterization methods described in the Section 2 are useful for this purpose. The resulting optimization methods are commonly known as *direct* methods. The second family of solution approaches consists of satisfying the necessary conditions for optimality by iteratively solving simplified versions of the multi-point boundary value problem. This latter family of approaches is termed as *indirect* methods in the literature. Indirect methods are especially suitable for the derivation of explicit guidance laws. Solutions to the conflict resolution problem via trajectory parameterization will be discussed in this section. Conflict resolution guidance law derivation using indirect methods will be considered in Section 4.

Two versions of the direct conflict resolution technique are discussed in the following subsections. In Section 3.1, the conflict resolution problem is formulated as a single objective optimization problem. The Sequential Quadratic Programming (SQP) method [34] is used to solve the resulting optimization problem. The conflict resolution problem is formulated and solved as a multi-objective optimization problem in Section 3.2. The goal attainment method [24, 25] is used to obtain the solutions to the multi-objective optimization problem.

The computational techniques are discussed in Sections 3.1 and 3.2, followed by a discussion of the numerical results in Section 3.3. Solutions are obtained for conflict situations involving two, three, four and six aircraft. All the conflict resolution solutions are obtained using piecewise linear trajectory parameterization. Comparisons between the single objective conflict resolution solutions, and multi-objective solutions are also given in Section 3.3.

3.1. Conflict Resolution as A Single Objective Optimization Problem

Single objective formulation of the conflict resolution problem considers the sum of individual aircraft flight times and fuel consumption as the performance index. Starting from a set of nominal waypoint sequences, the objective is to synthesize trajectories that resolve conflicts while optimizing the performance index. As a second part of the single objective

optimization study, the performance index is re-cast as the sum of the integral deviations of each aircraft from their nominal trajectories. Inequality constraints are included for inter-aircraft distance, maximum and minimum velocities, maximum climb and descent rates, maximum and minimum altitudes, maximum roll angle, maximum and minimum load factors, and maximum and minimum thrust magnitudes. The nominal trajectories of each aircraft are specified in terms of a set of waypoints (x,y,h,t) . The present formulation of the trajectory optimization problem allows the waypoints to be constrained in a any desired manner. Physical characteristics of each aircraft such as mass, drag coefficient, and fuel consumption rate also included in the study.

The algebraic transformations that relate thrust, load factor, and roll angle to the acceleration components discussed in Section 2 are included in the formulation so as to permit the imposition of aircraft performance constraints without including the aircraft equations of motion. Trajectories are parameterized using the piecewise linear parameterization scheme discussed in Section 2. The optimization algorithm adjusts the trajectory parameters to resolve any existing conflicts while minimizing cost and meeting the aircraft performance constraints. The optimization problem is currently set up to accommodate a maximum of ten aircraft, although this can easily be increased if necessary.

Optimal trajectories are computed using the SQP method. The sequential quadratic programming method has been found highly effective in solving a wide variety of constrained nonlinear programming problems [34]. The SQP method solves optimization problems of the form:

$$\begin{aligned} & \text{minimize } f(x) \\ & \text{subject to } g(x) \leq 0 \end{aligned} \tag{10}$$

by approximating the performance index by a quadratic function, and the constraints by linear functions. The SQP method attempts to imitate the Newton's method, which is known to converge to the optimal solution in the least number of steps for quadratic problems. In expressions (10), $f(x)$ is a scalar objective function, $g(x)$ is a vector of constraint functions, and x is an n -vector of optimization parameters. The scalar Lagrangian function [34] is formed by adjoining the constraints to the objective function with a vector λ of Lagrange multipliers:

$$L(x, \lambda) = f(x) + \lambda^T g(x) \tag{11}$$

The next step is to form a quadratic approximation of this function and to linearize the constraints about the current solution vector. The approximate optimization problem then becomes:

$$\text{minimize } \frac{1}{2} \mathbf{p}^T \mathbf{H} \mathbf{p} + \nabla f^T \mathbf{p} \quad (12)$$

$$\text{subject to } \nabla g^T \mathbf{p} + g \leq 0 \quad (13)$$

The vector \mathbf{p} is the local approximation of the optimization parameters, \mathbf{H} is the Hessian matrix and ∇ denotes the gradient operation with respect to \mathbf{x} , evaluated at the current solution vector. This approximate problem (12), (13) is next solved using the Quadratic Programming (QP) algorithm [34]. The active set strategy is used for constraint satisfaction. The first step in solving the minimization problem is to find a feasible starting point. Such a point can often be found using a linear programming algorithm with the linearized constraints. Failing that, a search can be performed in the direction of decreasing constraint violations. The feasible point determines the set of active constraints. A search direction \mathbf{d} is then calculated using the active constraints, and a one-dimensional line search is performed to minimize (12). A step is taken along the search direction \mathbf{d} , with a step length α .

$$\mathbf{x}_{i+1} = \mathbf{x}_i + \alpha \mathbf{d} \quad (14)$$

For quadratic problems it can be shown that the minimum occurs when $\alpha = 1$ as long as the constraints are not violated. Otherwise, smaller steps have to be taken and a new active set should be defined. However, due to the approximate nature of the QP problem, a more effective method is to use the solution of the QP problem as a direction and minimize a merit function which takes the inactive constraints also into consideration. The function employed in the present research is from Reference 35:

$$\psi(\mathbf{x}) = f(\mathbf{x}) + \sum_i r_i \max\{0, g_i(\mathbf{x})\} \quad (15)$$

where r_i are weighting parameters. Having found the appropriate step size, the new parameter vector x is found and a new approximate quadratic problem is formed and solved. The optimization toolbox of the MATLAB® software [36] is used in the present investigation for implementing the sequential quadratic programming algorithm.

An interesting aspect of the single objective conflict resolution method using the SQP algorithm is that the sensitivity of the cost function and constraints with respect to individual trajectory parameters can be readily computed using the gradient of the cost ∇f , Hessian matrix H , and the Jacobian matrix of the constraints ∇g . These sensitivities can be then used by individual aircraft to further negotiate changes to their path. For instance, large trajectory changes can be made in regions of low cost/constraint sensitivity, while trajectory perturbations must be limited in the high sensitivity regions. Such information can be valuable for the practical implementation of the conflict resolution method.

Numerical results using the single objective formulation of the conflict resolution problem will be given in Section 3.3. An alternate formulation of the conflict resolution problem is discussed in the following section.

3.2. Conflict Resolution As A Multiple Objective Optimization Problem

Single objective formulation of the conflict resolution problem is difficult to justify in the free-flight environment, because individual aircraft involved in the maneuvers may not be interested in optimizing a single performance index. For instance, some of the aircraft may place larger emphasis on flight time than fuel, while other aircraft may be interested in minimizing fuel consumption. Multiple objective optimization methods allow the use of more than one cost function, and are perhaps more realistic in representing the true nature of the multi-aircraft conflict resolution problem. Note that the multiple objective formulation automatically allows the simultaneous inclusion of cooperating and competing objectives, if any are present in the problem.

The cost function in the multi-objective conflict resolution problem is a vector. Several algorithms have been reported in the literature for the solution of multiple objective optimization problems [24]. Multiple objective optimization problems seek a set of “non-inferior” points as their solution. Non-inferiority implies that any further improvement in one objective would result in a degradation in another objective. Thus, all points in the solution set minimize the performance objectives to the maximum possible extent. The technique selected for use in the

present research is the Goal Attainment method discussed in Reference 24. Here, the objectives and the constraints are all represented as goals to be satisfied, and the degree to which these goals are met are adjusted using weighting functions. The goal attainment formulation allows the imposition of inequality and equality constraints.

Mathematically, the goal attainment method can be stated as:

$$\text{minimize } \gamma, \text{ where } f(x) - w\gamma \leq f^* \quad (16)$$

Note that $f(x)$ is a vector which includes the cost functions and the constraints. The goals are contained in the vector f , and the weights are in the vector w . The scalar γ is a measure of how far away a solution point is from the goals. Thus, the term $w\gamma$ can be considered as the slackness in the problem. Individual weights capture the fact that in many design problems, a goal need not be met exactly and one is more interested in arriving at an optimal trade-off between conflicting objectives. The weighting vector defines the direction from the goal point to the feasible region. As γ is varied, the feasible region changes size, until the constraint boundaries converge to a solution point. One of the advantages of the goal attainment formulation is that it can be solved as a sequential quadratic programming problem. A difference arises, though, in the merit function used for the line search. There are again several possibilities, but the one employed in the present research is from Reference 25:

$$\Psi(x) = \max_i \left\{ \frac{f_i(x) - f_i^*}{w_i} \right\} \quad (17)$$

Conflict resolution trajectories involving two, three, four and six aircraft have been generated using the goal attainment method. Some of these will be illustrated in Section 3.3.

3.3. Conflict Resolution Results

Conflict resolution methods developed in Sections 3.1 and 3.2 are evaluated in a sample conflict scenario in this section. The results for single objective and multiple objective formulations corresponding a six aircraft conflict will be given here.

This conflict scenario is generated by including six merging aircraft, five of them flying at 30,000 feet , and the sixth aircraft merging from 32,000 feet altitude. Such a conflict can arise during merging operations near an air traffic control center.

The initial aircraft speeds are:

$$V_1 = 780 \text{ ft/s}, V_2 = 733 \text{ ft/s}, V_3 = 548 \text{ ft/s}, V_4 = 708 \text{ ft/s}, V_5 = 586 \text{ ft/s}, V_6 = 490 \text{ ft/s}.$$

The aircraft parameters used in this conflict scenario are:

$$\text{Mass} = 185,000 \text{ lb}, \text{ Drag coefficient } (C_D) = 0.05, \text{ Wing area } (S) = 1700 \text{ ft}^2$$

Fuel consumption rate is assumed be a quadratic function of airspeed, with the constant of proportionality being $0.3 \times 10^{-6} \text{ lb}_m \cdot \text{sec} / \text{ft}^2$. The performance constraints imposed on the conflict resolution problem are:

$$340 \text{ ft/sec} < \text{Airspeed} < 900 \text{ ft/sec}$$

$$0.9 \text{ g's} < \text{Load Factor} < 1.1 \text{ g's}$$

$$1,000 \text{ lb}_f < \text{Thrust} < 48,000 \text{ lb}_f$$

$$20,000 \text{ ft} < \text{Altitude} < 40,000 \text{ ft}$$

$$-3,000 \text{ ft/min} < \text{Rate of Climb} < 1,000 \text{ ft/min}$$

The arrival order at the end of the maneuvers are assumed to be specified. Nominal trajectories for the aircraft are given Figure 4. It may be observed from the inter-aircraft distance plot that the conflicts between aircraft occur right from the beginning, and by 300 seconds, every aircraft is in conflict with the rest. Note that the conflict resolution strategies are far from obvious in this situation.

Conflict resolution using single objective formulation is given in Figure 5. Square of the deviations from nominal trajectories is used as the performance index in these optimization runs. Note that the methodology has modified each aircraft trajectory sufficiently to completely resolve the conflicts. Trajectory corrections have been introduced in both vertical plane and horizontal plane. Conflict resolution using multiple objective formulation is shown in Figure 6. Although it is rather difficult to gauge the differences between the two approaches, an analysis of the sensitivities of the trajectories with respect to the constraints show that the multiobjective formulation results in a more robust solution.

4. Closed-Loop Guidance Law for Conflict Resolution

The previous section discussed iterative techniques for conflict resolution. The conflict resolution problem will be formulated as a closed-loop guidance problem in this section. Guidance laws are developed based on the assumption that the nominal paths are the desirable paths, and that any perturbation from these paths should only be made to achieve conflict resolution. The guidance law derivation for two aircraft will be illustrated in this paper. Generalization to multiple aircraft conflicts is a future research item. From a guidance law derivation point-of-view, the aircraft involved in a potential conflict can act in the three following fashions.

- a) All aircraft involved in the potential conflict cooperate with each other for resolving the conflict. This would be the case when every aircraft is aware of every other aircraft in the vicinity, no aircraft has any priority over other aircraft, and all aircraft have comparable maneuverabilities. The resulting conflict resolution process will be termed here as *cooperative conflict resolution*.

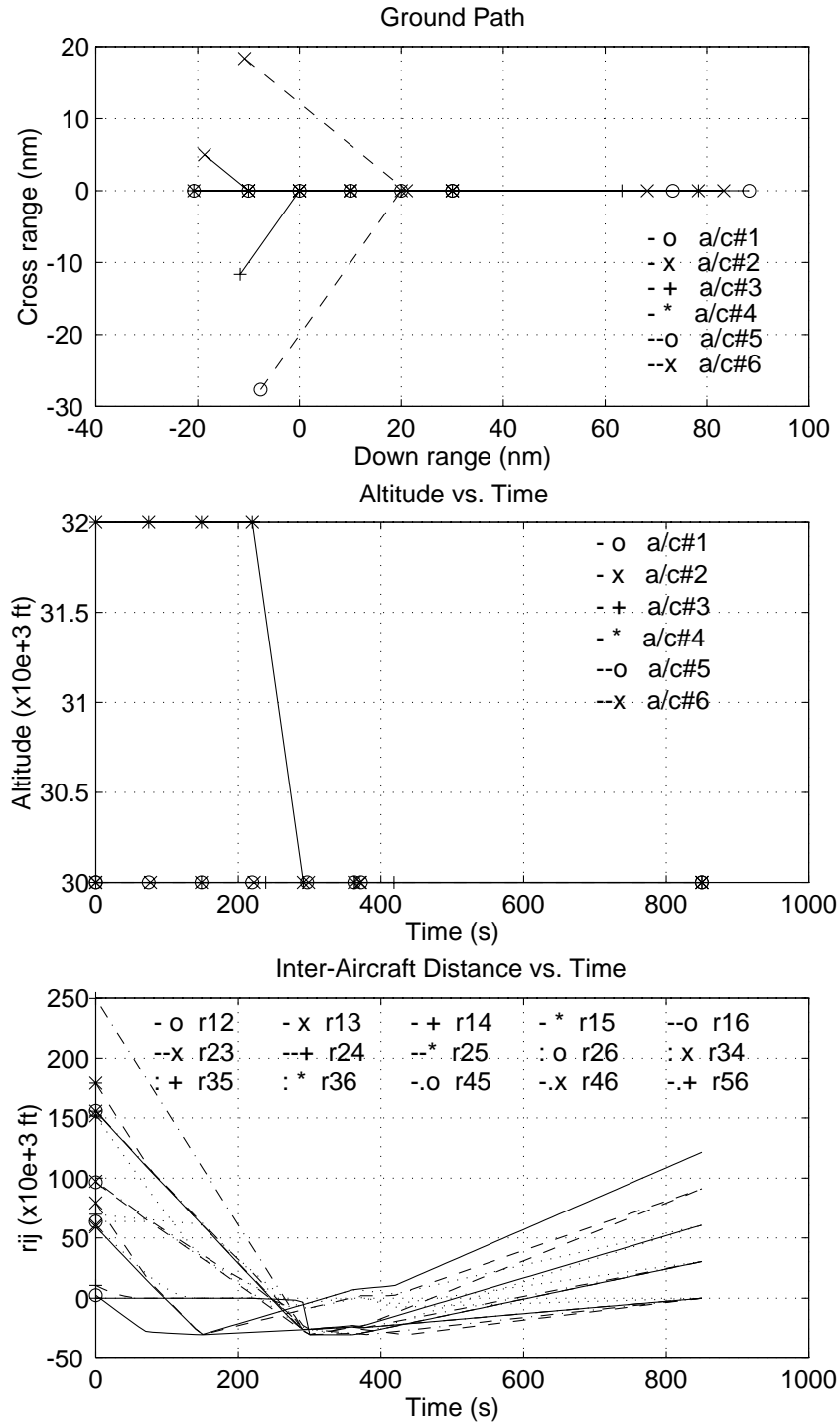


Fig. 4. Nominal Trajectories for Six Aircraft Conflict Resolution



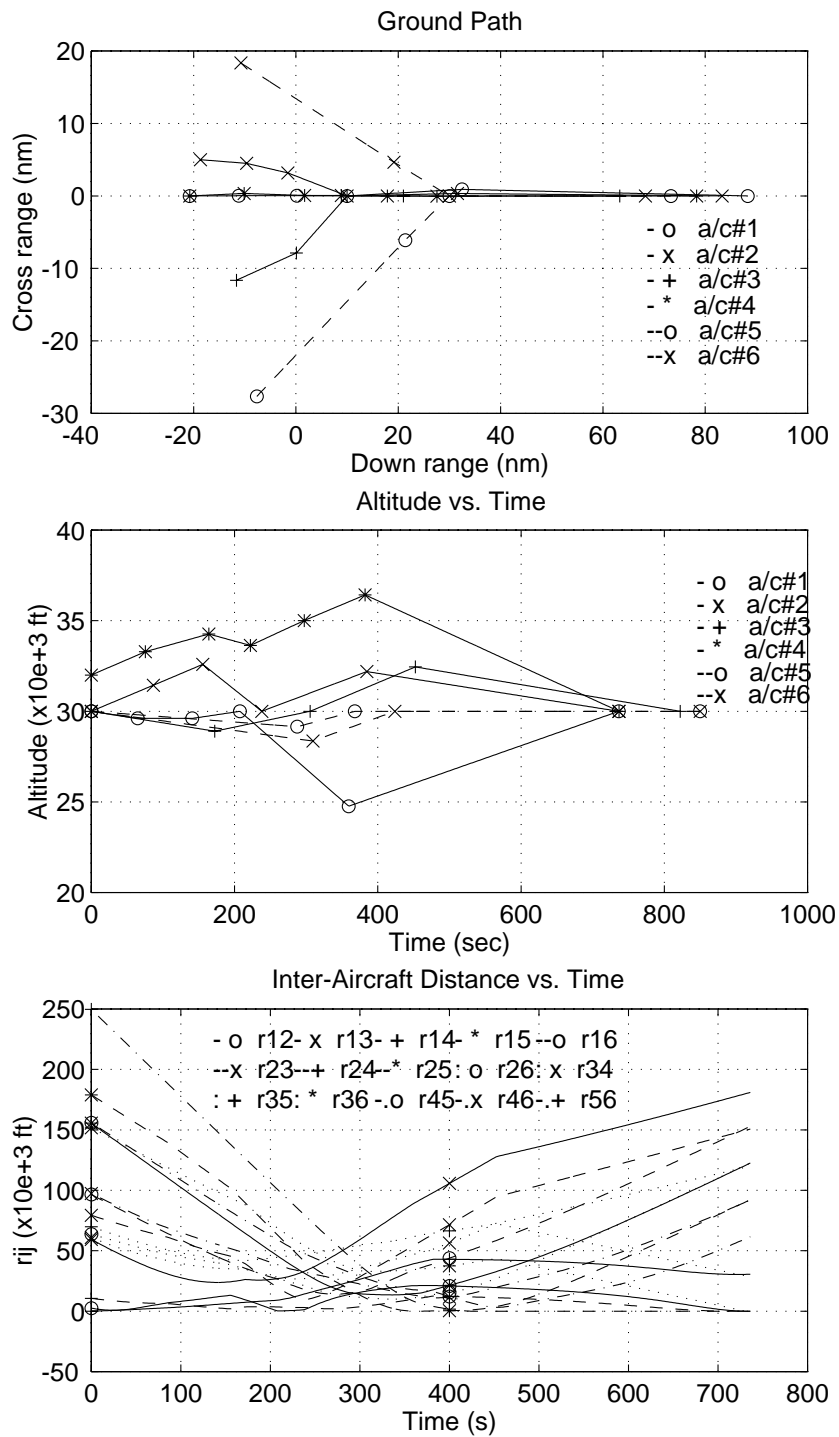


Fig. 5. Single Objective Conflict Resolution For the Six Aircraft Geometry



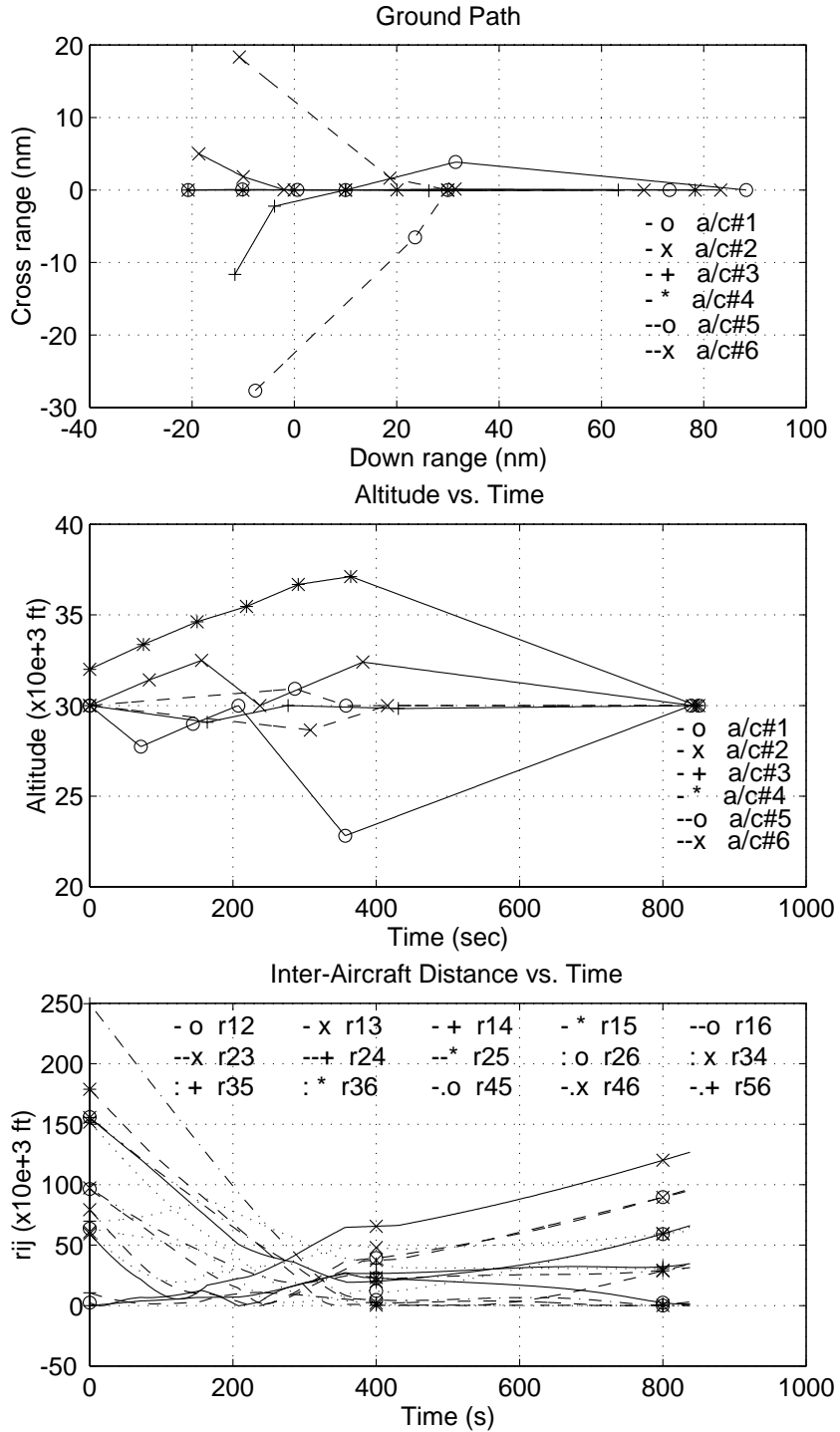


Fig. 6. Multiple Objective Conflict Resolution For the Six Aircraft Geometry

b) Some aircraft involved in the potential conflict continue to fly nominal paths, while others take on the responsibility for resolving the conflicts. This situation can arise

because of three distinct reasons. Firstly, some of the aircraft may be significantly more agile than other aircraft. In this case, the agile aircraft may be able to resolve conflicts much faster, and more efficiently than non-agile aircraft. The second mechanism for such a scenario is when the aircraft are assigned a priority ordering, such that certain aircraft are allowed to stay on their nominal trajectories, while the others are made responsible for conflict resolution. The third situation where this might occur is when some of the aircraft are not aware of other aircraft in the vicinity, and hence continue on their nominal paths, while the remaining aircraft have to take responsibility for conflict resolution. These scenarios can be termed as *noncooperative* conflict resolution.

- c) The third operational mode corresponds to the case of some of the aircraft in the airspace maneuvering in such a way as to increase the potential for conflict. This situation may arise whenever some of the aircraft are not aware of other aircraft in the vicinity, and may maneuver in such a way as to increase the conflicts. Alternatively, in order to assure guaranteed conflict resolution, each properly equipped aircraft in the vicinity may decide to maneuver under the assumption that the unequipped aircraft in the vicinity may alter their trajectories in such a way as to cause conflicts. This case will be termed here as *adversarial* or *competitive* conflict resolution. Note this conflict scenario has a solution only if the conflict-resolving aircraft have superior data gathering and maneuvering capabilities when compared with the adversarial aircraft.

Characterizing the conflict resolution problem in terms of these categories serves to capture the degree of optimism of the aircraft involved in a given conflict scenario. Thus, the first mode corresponds to fully optimistic conflict resolution process, while the second is more neutral. The third formalism is pessimistic, and will lead to highly conservative conflict resolution maneuvers.

Guidance law development will assume that each aircraft in the airspace has selected a nominal waypoint sequence based on some other criteria. The criteria for nominal trajectory selection may include the minimization of flight time and fuel consumption to reach a selected set of final conditions while satisfying aircraft and environmental constraints. They may also be based on prevailing atmospheric conditions, and the need for coordinating operations with other aircraft in the air transportation system. Conflict resolution guidance laws introduce perturbations on these nominal waypoints to resolve the conflicts. Conflict resolution perturbations can be

introduced in several different ways. For instance, the trajectory perturbations can be based on a set of rules capturing the maneuvering strategies in every given conflict situation. Alternatively, one may cast the trajectory perturbation problem as an optimal control problem [16] that minimizes the deviations from the nominal trajectories while achieving conflict resolution. In this framework, penalties can be placed on the magnitudes of acceleration, velocity, and position components. This approach is followed in the present research.

In order to formulate the conflict resolution problem in this manner, perturbations in each aircraft trajectory are first expressed as:

$$\delta x_1 = x_1 - \bar{x}_1, \delta y_1 = y_1 - \bar{y}_1, \delta z_1 = z_1 - \bar{z}_1 \quad (18)$$

$$\delta x_2 = x_2 - \bar{x}_2, \delta y_2 = y_2 - \bar{y}_2, \delta z_2 = z_2 - \bar{z}_2 \quad (19)$$

An over-bar denotes nominal values. Differentiating the expressions (18) and (19) twice with respect to time leads to the perturbed equations of motion:

$$\begin{aligned} \delta \ddot{x}_1 &= \ddot{x}_1 - \ddot{\bar{x}}_1 = u_1, & \delta \ddot{x}_2 &= \ddot{x}_2 - \ddot{\bar{x}}_2 = u_2 \\ \delta \ddot{y}_1 &= \ddot{y}_1 - \ddot{\bar{y}}_1 = v_1, & \delta \ddot{y}_2 &= \ddot{y}_2 - \ddot{\bar{y}}_2 = v_2 \\ \delta \ddot{z}_1 &= \ddot{z}_1 - \ddot{\bar{z}}_1 = w_1, & \delta \ddot{z}_2 &= \ddot{z}_2 - \ddot{\bar{z}}_2 = w_2 \end{aligned} \quad (20)$$

where $u_1, u_2, v_1, v_2, w_1, w_2$ are the perturbations in the aircraft acceleration components along down range, cross-range and altitude directions. These quantities can be related to perturbations in actual control variables of the aircraft using the expressions derived in Section 2. The reference values of the velocity and position components along the nominal trajectory can be determined using the given waypoint sequence.

Deviations from nominal trajectory can be characterized in terms of the Euclidean norm of the perturbations on velocity and position perturbations. The position perturbations are not included in the performance index used in the present research. Thus, a performance index of the form:

$$\min_{u_1, u_2, v_1, v_2, w_1, w_2} \frac{1}{2} \int_0^{t_f} \left[\alpha_1^2 (\delta \dot{x}_1^2 + \delta \dot{y}_1^2 + \delta \dot{z}_1^2) + \alpha_2^2 (\delta \dot{x}_2^2 + \delta \dot{y}_2^2 + \delta \dot{z}_2^2) + \frac{1}{\beta_1^2} (u_1^2 + v_1^2 + w_1^2) + \frac{1}{\beta_2^2} (u_2^2 + v_2^2 + w_2^2) \right] dt \quad (21)$$

is used for the conflict resolution problem. Weighting factors α_1 , β_1 , α_2 , β_2 can be used to adjust the relative importance of velocity and acceleration perturbations. They can also be used to cast the problem as cooperative, noncooperative or adversarial conflict resolution problem. For instance, using equal weights for both aircraft will result in cooperative conflict resolution, while using very large weights for one of the aircraft will produce the noncooperative conflict resolution solution. Changing the signs of the terms for one of the aircraft in the performance index will produce the adversarial conflict resolution solution. For the sake of illuminating the guidance law development, the present research will employ equal weighting factors for both aircraft. In this case, the weighting factors on the perturbed velocity components can be used to scale the weighting factor on the acceleration components. Other conflict resolution guidance laws will be more fully explored during future research.

Since the conflict resolution perturbations must begin and end on the nominal trajectories, they must satisfy the boundary conditions:

$$\begin{aligned} \delta x_1(0) = \delta \dot{x}_1(0) = \delta x_2(0) = \delta \dot{x}_2(0) = 0 \\ \delta x_1(t_f) = \delta \dot{x}_1(t_f) = \delta x_2(t_f) = \delta \dot{x}_2(t_f) = 0 \end{aligned} \quad (22)$$

The minimum inter-aircraft distance requirement between the two aircraft at the time of conflict can be expressed as an interior-point equality constraint of the form:

$$\begin{aligned} (\bar{x}_1 + \delta x_1 - \bar{x}_2 - \delta x_2)^2 + (\bar{y}_1 + \delta y_1 - \bar{y}_2 - \delta y_2)^2 + (\bar{z}_1 + \delta z_1 - \bar{z}_2 - \delta z_2)^2 \\ - (\bar{x}_1 - \bar{x}_2)^2 - (\bar{y}_1 - \bar{y}_2)^2 - (\bar{z}_1 - \bar{z}_2)^2 \Big|_{t=t_c} = R_{\min}^2 \end{aligned} \quad (23)$$

Or:

$$\begin{aligned} (\delta x_1 - \delta x_2)^2 + (\delta y_1 - \delta y_2)^2 + (\delta z_1 - \delta z_2)^2 \\ + 2(\bar{x}_1 - \bar{x}_2)(\delta x_1 - \delta x_2) + 2(\bar{y}_1 - \bar{y}_2)(\delta y_1 - \delta y_2) + 2(\bar{z}_1 - \bar{z}_2)(\delta z_1 - \delta z_2) \Big|_{t=t_c} = R_{\min}^2 \end{aligned} \quad (24)$$

A conflict is assumed to have been detected at time t_c , and R_{\min} is the desired additional separation distance between the two aircraft at the point-of-closest approach. It is assumed that : $0 \bullet t_c \bullet t_r$. In the case of n conflicting aircraft, the optimal trajectories will have to satisfy $n(n-1)/2$ constraints of this form.

Additionally, in order to ensure that the separation between the aircraft does not decrease after t_c , the relative velocity along the direction of minimum separation will be required to satisfy the additional interior-point constraint:

$$\begin{aligned} & (\delta x_1 - \delta x_2)(\delta \dot{x}_1 - \delta \dot{x}_2) + (\delta y_1 - \delta y_2)(\delta \dot{y}_1 - \delta \dot{y}_2) + (\delta z_1 - \delta z_2)(\delta \dot{z}_1 - \delta \dot{z}_2) \\ & + (\dot{\bar{x}}_1 - \dot{\bar{x}}_2)(\delta x_1 - \delta x_2) + (\bar{x}_1 - \bar{x}_2)(\delta \dot{x}_1 - \delta \dot{x}_2) + (\dot{\bar{y}}_1 - \dot{\bar{y}}_2)(\delta y_1 - \delta y_2) + (\bar{y}_1 - \bar{y}_2)(\delta \dot{y}_1 - \delta \dot{y}_2) \\ & + (\dot{\bar{z}}_1 - \dot{\bar{z}}_2)(\delta z_1 - \delta z_2) + (\bar{z}_1 - \bar{z}_2)(\delta \dot{z}_1 - \delta \dot{z}_2) \Big|_{t=t_c} = 0 \end{aligned} \quad (25)$$

In the interests of maintaining simplicity, for this initial study, the conflict envelope has been assumed to spherical. The guidance law derivation along one of the coordinate axes will be illustrated in the following.

4.1. Conflict Resolution Guidance Law in the Down-Range Direction

In order to limit the complexity of the derivations in this initial research, it will be assumed that the conflict resolution problem can be solved independently along each coordinate direction by generating the identical amounts of separation along each axis. For instance, a performance index of the form:

$$\min_{u_1, u_2} \frac{1}{2} \int_0^{t_f} \left[(\delta \dot{x}_1^2 + \delta \dot{x}_2^2) + \frac{1}{\beta^2} (u_1^2 + u_2^2) \right] dt \quad (26)$$

is used in the down range direction. Similar performance indices can be used along the cross range and altitude directions. The interior point equality constraints are then expressed as:

$$\left[(\delta x_1 - \delta x_2)^2 + 2(\bar{x}_1 - \bar{x}_2)(\delta x_1 - \delta x_2) \right]_{t=t_c} = r_{\min}^2 \quad (27)$$

$$\left[(\delta x_1 - \delta x_2)(\delta \dot{x}_1 - \delta \dot{x}_2) + (\dot{\bar{x}}_1 - \dot{\bar{x}}_2)(\delta x_1 - \delta x_2) + (\bar{x}_1 - \bar{x}_2)(\delta \dot{x}_1 - \delta \dot{x}_2) \right]_{t=t_c} = 0 \quad (28)$$

where r_{\min} is the additional separation to be generated along the down range direction. Note that the second interior point constraint further simplifies to $(\delta\dot{x}_1 - \delta\dot{x}_2) = 0$, if $(\dot{\bar{x}}_1 - \dot{\bar{x}}_2) = 0$ at $t=t_c$.

Optimal control problems with interior-point constraints can be treated as two distinct optimal control problems, the first one defined in the interval $[0, t_c]$ with the interior point constraints as the terminal conditions, while the second optimal control problem is defined in the interval $[t_c, t_f]$ with interior point constraints as the initial conditions.

The solution to the second problem will be discussed first because it is easier to solve. Define the variational Hamiltonian [16] as

$$H = \frac{1}{2} \left[(\delta\dot{x}_1^2 + \delta\dot{x}_2^2) + \frac{1}{\beta^2} (u_1^2 + u_2^2) \right] + \lambda_1 u_1 + \lambda_2 u_2 + \lambda_3 \delta\dot{x}_1 + \lambda_4 \delta\dot{x}_2 \quad (29)$$

The Euler-Lagrange Equations are of the form:

$$\dot{\lambda}_1 = -\delta\dot{x}_1 - \lambda_3, \dot{\lambda}_3 = 0, u_1 = -\beta^2 \lambda_1 \quad (30)$$

$$\dot{\lambda}_2 = -\delta\dot{x}_2 - \lambda_4, \dot{\lambda}_4 = 0, u_2 = -\beta^2 \lambda_2 \quad (31)$$

The first two sets of costate equations and optimality conditions can be solved in closed-form as:

$$\lambda_1 = a_1 e^{\beta t} + b_1 e^{-\beta t}, u_1 = -\beta^2 (a_1 e^{\beta t} + b_1 e^{-\beta t}) \quad (32)$$

$$\lambda_2 = a_2 e^{\beta t} + b_2 e^{-\beta t}, u_2 = -\beta^2 (a_2 e^{\beta t} + b_2 e^{-\beta t}) \quad (33)$$

where a_1, b_1, a_2, b_2 are the arbitrary constants in the solution. The expressions for optimal control are next substituted in the equations of motion and integrated to yield:

$$\delta\dot{x}_1 = c_1 - \beta (a_1 e^{\beta t} - b_1 e^{-\beta t}), \delta\dot{x}_2 = c_2 - \beta (a_2 e^{\beta t} - b_2 e^{-\beta t}) \quad (34)$$

$$\delta x_1 = d_1 + c_1 t - (a_1 e^{\beta t} + b_1 e^{-\beta t}), \delta x_2 = d_2 + c_2 t - (a_2 e^{\beta t} + b_2 e^{-\beta t}) \quad (35)$$

where c_1, c_2, d_1, d_2 are arbitrary constants in the solution. Using these expressions, the costates λ_3, λ_4 can be found to be:

$$\lambda_3 = -c_1, \lambda_4 = -c_4 \quad (36)$$

The arbitrary constants $a_1, b_1, c_1, d_1, a_2, b_2, c_2, d_2$ can be evaluated using the given boundary conditions. Applying the boundary conditions at t_c and t_f yields the expressions:

$$a_1 \left(1 - e^{\beta(t_f - t_c)}\right) - b_1 \left(1 - e^{-\beta(t_f - t_c)}\right) = \frac{\delta \dot{x}_1(t_f) - \delta \dot{x}_1(t_c)}{\beta} \quad (37)$$

$$a_2 \left(1 - e^{\beta(t_f - t_c)}\right) - b_2 \left(1 - e^{-\beta(t_f - t_c)}\right) = \frac{\delta \dot{x}_2(t_f) - \delta \dot{x}_2(t_c)}{\beta} \quad (38)$$

$$a_1 \left[1 + \beta(t_f - t_c) - e^{\beta(t_f - t_c)}\right] + b_1 \left[1 - \beta(t_f - t_c) - e^{-\beta(t_f - t_c)}\right] = \delta x_1(t_f) - \delta x_1(t_c) - [t_f - t_c] \delta \dot{x}_1(t_c) \quad (39)$$

$$a_2 \left[1 + \beta(t_f - t_c) - e^{\beta(t_f - t_c)}\right] + b_2 \left[1 - \beta(t_f - t_c) - e^{-\beta(t_f - t_c)}\right] = \delta x_2(t_f) - \delta x_2(t_c) - [t_f - t_c] \delta \dot{x}_2(t_c) \quad (40)$$

$$c_1 = \delta \dot{x}_1(t_c) + \beta(a_1 - b_1), d_1 = \delta x_1(t_c) + (a_1 + b_1) \quad (41)$$

$$c_2 = \delta \dot{x}_2(t_c) + \beta(a_2 - b_2), d_2 = \delta x_2(t_c) + (a_2 + b_2) \quad (42)$$

These expressions can be solved to obtain the trajectory perturbations required to restore the aircraft to the nominal trajectories after conflict resolution.

In order to handle the state constrained optimal control problem between the initial time and the point of closest approach, define

$$\begin{aligned} \Phi(t_c) = & \mu_1 \left[(\delta x_1 - \delta x_2)^2 + 2(\bar{x}_1 - \bar{x}_2)(\delta x_1 - \delta x_2) \Big|_{t=t_c} - r_{\min}^2 \right] \\ & + \mu_2 \left[(\delta x_1 - \delta x_2)(\delta \dot{x}_1 - \delta \dot{x}_2) + (\dot{\bar{x}}_1 - \dot{\bar{x}}_2)(\delta x_1 - \delta x_2) + (\bar{x}_1 - \bar{x}_2)(\delta \dot{x}_1 - \delta \dot{x}_2) \Big|_{t=t_c} \right] \end{aligned} \quad (43)$$

μ_1 and μ_2 are two undetermined constants. The condition (4.28) imposes constraints on the value of the costates at $t = t_c$ as:

$$\lambda_1(t_c) = \mu_2 \left[(\delta x_1 - \delta x_2) + (\bar{x}_1 - \bar{x}_2) \Big|_{t=t_c} \right] \quad (44)$$

$$\lambda_2(t_c) = -\mu_2 \left[(\delta x_1 - \delta x_2) + (\bar{x}_1 - \bar{x}_2) \Big|_{t=t_c} \right] \quad (45)$$

implying: $\lambda_1(t_c) = -\lambda_2(t_c)$. This leads to the result:

$$(a_1 + a_2)e^{\beta t_c} = -(b_1 + b_2)e^{-\beta t_c} \quad (46)$$

Similarly,

$$\lambda_3(t_c) = \mu_1 \left[2(\delta x_1 - \delta x_2) + 2(\bar{x}_1 - \bar{x}_2) \Big|_{t=t_c} \right] + \mu_2 \left[(\delta \dot{x}_1 - \delta \dot{x}_2) + (\dot{\bar{x}}_1 - \dot{\bar{x}}_2) \Big|_{t=t_c} \right] \quad (47)$$

$$\lambda_4(t_c) = -\mu_1 \left[2(\delta x_1 - \delta x_2) + 2(\bar{x}_1 - \bar{x}_2) \Big|_{t=t_c} \right] - \mu_2 \left[(\delta \dot{x}_1 - \delta \dot{x}_2) + (\dot{\bar{x}}_1 - \dot{\bar{x}}_2) \Big|_{t=t_c} \right] \quad (48)$$

which implies $\lambda_3(t_c) = -\lambda_4(t_c)$. Substituting for these quantities:

$$(a_1 + a_2) - (b_1 + b_2) = \frac{-\delta \dot{x}_2(0) - \delta \dot{x}_1(0)}{\beta} \quad (49)$$

These equations can be used to obtain:

$$(b_1 + b_2) = \frac{\delta \dot{x}_2(0) + \delta \dot{x}_1(0)}{\beta(1 + e^{-2\beta t_c})}, (a_1 + a_2) = - \left[\frac{\delta \dot{x}_2(0) + \delta \dot{x}_1(0)}{\beta(1 + e^{-2\beta t_c})} \right] e^{-2\beta t_c} \quad (50)$$

The terminal constraints yield the following relationships:

$$(\delta x_1 - \delta x_2) \Big|_{t=t_c} = -(\bar{x}_1 - \bar{x}_2) \pm \sqrt{(\bar{x}_1 - \bar{x}_2)^2 + r_{\min}^2} \Big|_{t=t_c} \quad (51)$$

$$(\delta \dot{x}_1 - \delta \dot{x}_2) \Big|_{t=t_c} = \frac{-(\dot{\bar{x}}_1 - \dot{\bar{x}}_2) \left[-(\bar{x}_1 - \bar{x}_2) \pm \sqrt{(\bar{x}_1 - \bar{x}_2)^2 + r_{\min}^2} \right]}{\pm \sqrt{(\bar{x}_1 - \bar{x}_2)^2 + r_{\min}^2}} \Big|_{t=t_c} \quad (52)$$

From closed-form solutions,

$$(\delta \dot{x}_1 - \delta \dot{x}_2) \Big|_{t=t_c} = c_1 - c_2 - \beta(a_1 - a_2)e^{\beta t_c} + \beta(b_1 - b_2)e^{-\beta t_c}$$

(53)

$$(\delta x_1 - \delta x_2) \Big|_{t=t_c} = d_1 - d_2 + (c_1 - c_2)t_c - (a_1 - a_2)e^{\beta t_c} - (b_1 - b_2)e^{-\beta t_c}$$

(54)

Next substituting for the arbitrary constants in terms of the boundary conditions,

$$(\delta \dot{x}_1 - \delta \dot{x}_2) \Big|_{t=t_c} = [\delta \dot{x}_1(0) - \delta \dot{x}_2(0)] + (a_1 - a_2)\beta [1 - e^{\beta t_c}] - (b_1 - b_2)\beta [1 - e^{-\beta t_c}]$$

(55)

$$\begin{aligned} (\delta x_1 - \delta x_2) \Big|_{t=t_c} &= [\delta x_1(0) - \delta x_2(0)] + [\delta \dot{x}_1(0) - \delta \dot{x}_2(0)]t_c + (a_1 - a_2)[1 + \beta t_c - e^{\beta t_c}] \\ &+ (b_1 - b_2)[1 - \beta t_c - e^{-\beta t_c}] \end{aligned}$$

(56)

These two equations can be solved for $(a_1 - a_2)$ and $(b_1 - b_2)$. They can then be combined with the expressions for $(a_1 + a_2)$ and $(b_1 + b_2)$ to yield the arbitrary constants a_1, b_1, a_2, b_2 . These can then be used to determine the remaining constants in the problem c_1, d_1, c_2, d_2 .

This completes the computation of the perturbations required to resolve conflicts. These perturbations can be added to the nominal paths to yield the conflict resolved trajectories. Note that the perturbation equations are solved from the current time to the final time in every guidance interval.

These perturbations correct the nominal waypoints to form the new waypoint sequence. Note that the addition of the perturbations to the nominal may not always resolve the conflict. In highly nonlinear geometries, the conflict resolution computations will have to be repeated several times to generate conflict-free waypoint sequences. In these cases, it is beneficial to multiply the perturbations by an attenuating factor before adding to the nominal trajectories. The resulting algorithm will turn out to be the quasi-linearization technique [16, 38] or the technique of invariant embedding. Quasilinearization is a second-order technique and is known to converge rapidly to the optimal solution.

The conflict resolution algorithm is next evaluated for a set of conflict scenarios involving two aircraft. These simulation results are given in the next subsection.

4.2. Simulation Results

A two-aircraft conflict scenario is chosen to demonstrate the guidance law performance. In all cases, the weighting factor β is chosen to be 10^{-03} . The conflict resolution case considered is

that of two aircraft with crossing trajectories. Figure 7 illustrates the down range-cross range trajectories, altitude profiles and inter-aircraft distances before and after the conflict resolution maneuvers. The trajectories before conflict resolution are denoted by dashed lines, and the trajectories after conflict resolution are denoted using dashed lines. Since cooperative conflict resolution is assumed, both aircraft perform conflict resolution maneuvers as can be observed in the down range - cross range plot. Due to the assumption that equal amounts of conflict resolution maneuvers will be made in the down range, cross range and altitude directions, the aircraft also perform maneuvers in the vertical plane. It can be observed from the inter-aircraft distance shown in Figure 7 that each aircraft has adjusted its trajectory to resolve the conflict.

In the present example, the guidance problem was solved as a quasilinearization problem. In the quasilinearization formulation, the trajectory perturbations generated by the guidance law are attenuated before being added to the nominal trajectories. The updated nominal trajectory is then used to compute the conflict resolution trajectory perturbations. Iterative computations are continued until the conflict is resolved. In the present case, a perturbation factor of 0.2 is used, and the solution converged in three iterations.

The simulation results presented in this subsection illustrate the performance capabilities of the conflict resolution guidance law. In each case, the guidance law resolves the conflicts using modest control magnitudes. As indicated elsewhere in this chapter, the guidance law can be extended to include multiple aircraft executing widely different nominal trajectories. Moreover, inequality constraints can be imposed on the control magnitudes to improve the implementability of the present guidance laws. The ride-quality of these conflict resolution guidance laws can be further improved by introducing control rate limits. This will produce smooth control settings, resulting in nearly jerk-free trajectories. Finally, the present formulation can be extended to the spherical earth case. The kinematic trajectory models of the form given in Reference 4 can be readily adapted for this purpose.

The derivations presented in this chapter, together with the simulation results amply demonstrate the feasibility of developing on-board implementable guidance laws for conflict resolution in free flight.

5. Conclusions

This paper documented the results of a research study that examined development of advanced algorithms for air traffic conflict resolution. The research was motivated by the free flight concept currently being considered for implementation as a part of the national air traffic

control system. In the free flight concept, individual aircraft will be allowed to plan and execute their trajectories without direction from any external agents during most of their flight duration. However, since each aircraft in the airspace may have conflicting objectives, the desired trajectories synthesized by individual aircraft can produce conflicts with other aircraft trajectories. While conflict resolution strategies are obvious under low speed, low traffic density conditions, the problem can become complex as the traffic density and the aircraft speeds increase.

The conflict resolution problem was formulated and solved as a multi-participant optimal control problem in the present research. The problem was formulated under the assumption that the objective of each aircraft involved in a potential conflict is to optimize its performance while maintaining adequate separation between other aircraft in the vicinity. Point-mass aircraft models and oblate spheroidal conflict envelopes were

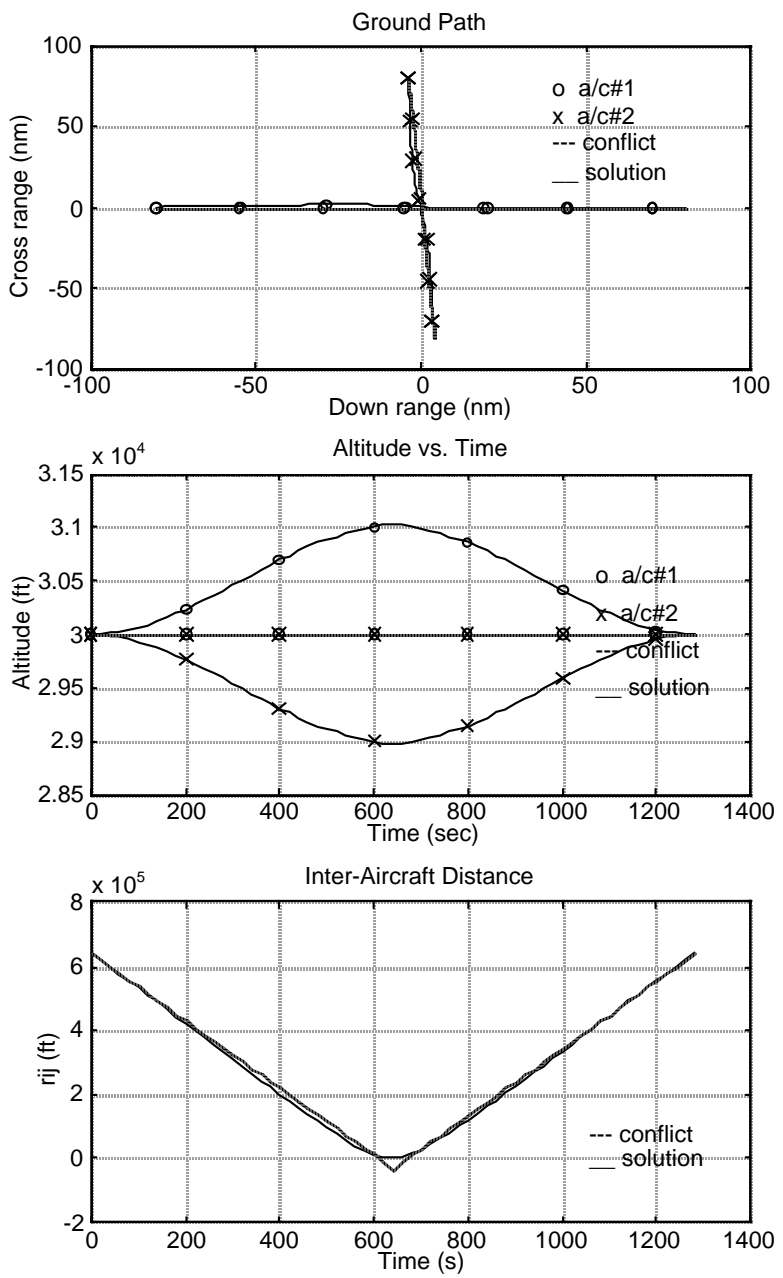


**Fig. 7. Conflict Resolution Trajectories Using
The Quasilinearization Guidance Law:
Crossing Trajectories**

used in this study. Point mass models included thrust, load factor, and bank angle as the control variables. Inequality constraints were imposed on the aircraft altitude, climb/descent rate, airspeed, and control magnitudes. The oblate spheroidal conflict envelope provided a smooth approximation to the FAA mandated separation between aircraft. The conflict envelope had a 5 nautical mile semi-major axis, and a 2000 feet semi-minor axis.

Two distinct approaches for solving the conflict resolution problem were advanced. In the first approach, the aircraft trajectories were approximated using piecewise linear curves to convert the trajectory optimization problems into parameter optimization problems. In the second approach, the aircraft equations of motion were linearized about the nominal trajectories, and state-constrained multi-point boundary value problems were formulated. Parameterized conflict resolution problems were solved using single objective sequential quadratic programming method, and a multiple objective goal attainment method. Conflict resolution involving six aircraft were demonstrated. State constrained multi-point boundary value problems were solved in closed-form to generate conflict resolution guidance laws. Performance of the guidance laws for several conflict scenarios were demonstrated.

6. References

1. Final Report of the RTCA Task Force 3: *Free Flight Implementation*, RTCA Inc., October 26, 1995.
2. Special Report on Free Flight, *Aviation Week and Space Technology*, July 31, 1995.
3. Bilimoria, K., Sridhar, B., and Chatterji, G., "Effects of Conflict Resolution Maneuvers and Traffic Density on Free Flight", *AIAA Guidance, Navigation, and Control Conference*, July 29-31, 1996, San Diego, CA.
4. Chatterji, G., Sridhar, B., and Bilimoria, K., "En-route Flight Trajectory Prediction for Conflict Avoidance and Traffic Management", *AIAA Guidance, Navigation, and Control Conference*, July 29-31, 1996, San Diego, CA.
5. Menon, P. K., "Control Theoretic Approach to Air Traffic Conflict Resolution", *Guidance, Navigation, and Control Conference*, August 9 -11, 1993, Monterey, CA.
6. Pritchett, A. R., and Hansman, R. J., "Experimental Study of Collision Detection Schema Used by Pilots During Closely Spaced Parallel Approaches", *AIAA Guidance, Navigation, and Control Conference*, July 29-31, 1996, San Diego, CA.

7. Slattery, R. A., "Terminal Area Trajectory Synthesis for Air Traffic Control Automation", *Proceedings of the 1995 American Control Conference*, Seattle, WA.
8. Krozel, J., Mueller, T., and Hunter, G., "Free Flight Conflict Detection and Resolution Analysis", *AIAA Guidance, Navigation, and Control Conference*, July 29-31, 1996, San Diego, CA.
9. Pujet, N., and Feron, E., "Flight Plan Optimization in Flexible Air Traffic Environments", *AIAA Guidance, Navigation, and Control Conference*, July 29-31, 1996, San Diego, CA.
10. Adams, M., Kolitz, S., and Odoni, A., "Evolutionary Concepts for Decentralized Air Traffic Flow Management", *AIAA Guidance, Navigation, and Control Conference*, July 29-31, 1996, San Diego, CA.
11. Erzberger, H., "CTAS: Integrated Automation Tools for the Center and TRACON", *The Journal of Air Traffic Control*, Oct. -Dec. 1990, Vol. 32, No. 4, pp. 90 - 91.
12. Erzberger, H., and Nedell, W., "Design of Automated System for Management of Arrival Traffic", NASA TM 102201, June 1989.
13. Erzberger, H., "CTAS: Computer Intelligence for Air Traffic Control in the Terminal Area", NASA Technical Memorandum 103959, July 1992.
14. Davis, T. J., Erzberger, H., Green, S. M., and Nedell, W., "Design and Evaluation of an Air Traffic Control Final Approach Spacing Tool", *Journal of Guidance, Control, and Dynamics*, Vol. 14, No. 4, July-Aug. 1991, pp. 848-854.
15. Davis, T. J., Erzberger, H., and Green, S. M., "Simulator Evaluation of the Final Approach Spacing Tool", NASA TM 102807, May 1990.
16. Bryson, A. E., and Ho, Y. C., *Applied Optimal Control*, Hemisphere, New York, 1975
17. Isaacs, R., *Differential Games*, R. E. Krieger, New York, 1965.
18. Menon, P. K. and Cheng, V. H. L., "Minimum-Exposure Near Terrain Flight Trajectories for Rotorcraft", Chapter 9 in *Control and Dynamic Systems* Edited by C. T. Leondes, Vol. 52, pp. 391 - 433.
19. Menon, P. K., Kim, E., and Cheng, V. H. L., "Helicopter Trajectory Planning Using Optimal Control Theory", *Proceedings of the 1988 American Control Conference*, Atlanta, GA, June 15 - 17, pp. 1440-1447.
20. Cheng, V. H. L., "Obstacle-Avoidance Automatic Guidance: A Concept Development Study", *AIAA Guidance, Navigation, and Control Conference*, Aug. 15 - 17, 1988, Minneapolis, MN.

21. Pekelsma, N. J., "Optimal Guidance with Obstacle Avoidance for Nap-of-the-Earth Flight", NASA CR 177515, December 1988.
22. Menon, P. K., Chatterji, G. B., and Sridhar, B., "Vision-Based Optimal Obstacle Avoidance Guidance for Rotorcraft", *Proceedings of the AIAA Guidance, Navigation, and Control Conference*, New Orleans, LA, August 1991.
23. Menon, P. K., "Air Traffic Conflict Resolution Using Modern Control Theory", *Optimal Synthesis* Report Prepared for NASA Ames Research Center under Subcontract No. 02804230, October 1992.
24. Gembicki, F. W., "Vector Optimization for Control with Performance and Parameter sensitivity Indices", *Ph.D Dissertation*, Case Western Reserve University, Cleveland, OH, 1974.
25. Brayton, R. K., Director, S. W., Hachtel, G. D., and Vidigal, L., "A New Algorithm for Statistical Circuit Design Based on Quasi-Newton Methods and Function Splitting", *IEEE Transactions on Circuits and Systems*, Vol. CAS-26, September 1979, pp. 784-794.
26. Nelson, R. C., *Flight Stability and Automatic Control*, McGraw-Hill Book Company, San Francisco, 1989.
27. Etkin, B., *Dynamics of Atmospheric Flight*, John Wiley, New York, NY, 1982.
28. Menon, P. K., "Short-Range Nonlinear Feedback Strategies for Aircraft Pursuit-Evasion", *Journal of Guidance, Control and Dynamics*, Vol. 12, January - February 1989, pp. 27 - 32.
29. Gerald, C. F., *Applied Numerical Analysis*, Addison Wesley, Reading, MA, 1978.
30. Kreyszig, E., *Advanced Engineering Mathematics*, Wiley, New York, New York, 1993.
31. Anon, *MATLAB[®] User's Manual*, The MathWorks, Inc., Natick, MA, 1994.
32. Barr, A. H., "Super Quadric Surfaces", *IEEE Transactions on Computer Graphics and Applications*, 1981.
33. Golub, G. H., and Van loan, C. F., *Matrix Computations*, The John Hopkins University Press, Baltimore, Maryland, 1989.
34. Gill, P. E., Murray, W. and Wright, M. H., *Practical Optimization*, Academic Press, New York, NY, 1981.
35. Dantzig, G., *Linear Programming and Extensions*, Princeton University Press, Princeton, NJ, 1963.
36. Grace, A., *Optimization Toolbox for MATLAB*, The MathWorks, Inc., Natick, MA, 1992.

37. Green, W., Swanborough, G., and Mowinski, J., *Modern Commercial Aircraft*, Crown Publishers, New York, NY, 1987.
38. Balakrishnan, A. V., and Neustadt, L. W. (Editors), *Computing Methods in Optimization Problems*, Academic Press, New York, NY, 1964.

